Cite this: *Phys. Chem. Chem. Phys.*, 2014, **16**, 12282

The angular overlap model extended for two-open-shell f and d electrons

Harry Ramanantoanina,[a] Werner Urland,*[ab] Fanica Cimpoesu*[c] and Claude Daul*[a]

We discuss the applicability of the Angular Overlap Model (AOM) to evaluate the electronic structure of lanthanide compounds, which are currently the subject of incredible interest in the field of luminescent materials. The functioning of phosphors is well established by the f–d transitions, which requires the investigation of both the ground $4f^n$ and excited $4f^{n-1}5d^1$ electron configurations of the lanthanides. The computational approach to the problem is based on the effective Hamiltonian adjusted from ligand field theory, but not restricted to it. The AOM parameterization implies the chemical bonding concept. Focusing our interest on this interaction, we take the advantages offered by modern computational tools to extract AOM parameters, which ensure the transparency of the theoretical determination and convey chemical intuitiveness of the non-empirical results. The given model contributes to the understanding of lanthanides in modern phosphors with high or low site symmetry and presents a non-empirical approach using a less sophisticated computational procedure for the rather complex problem of the ligand field of both 4f and 5d open shells.

Introduction

Before entering the central issues of our computational and modelling approaches we mention several topics where the simulation is important as a property engineering tool. The functioning of phosphor-converted-light-emitting-diodes (pc-LEDs) deserves strong interest since the ban on incandescent light bulbs. At the first stage of the development of LEDs, white light is produced by lanthanide Ce^{3+} doped inorganic phosphors,[1] taking advantages of the strong dipole allowed f–d transitions in Ce^{3+}.

Given the limit of the trial-and-error experiments of new phosphor synthesis, the future of our domestic lighting relies also on the theoretical modelling. The theoretical modelling gives the prospect of the optical manifestations of the phosphors together with a reliable understanding of their microscopic origin. *Ergo*, it contributes to the design of modern phosphors. Attention is particularly paid to the optical properties of the lanthanide ions Pr^{3+} or Eu^{2+} especially as activators for the warm-white light source.[2–4] The theoretical modelling of such phosphors is not free of puzzling technical concerns. Numerous studies related not only to the gigantic size-problem encountered,[5] like in the case of Eu^{2+}, but also the non-negligible issues due to low symmetry constraints.[6–8] We mention also the situation of non-aufbau occupation[9–12] of the 4f orbitals inasmuch as convergence problems may frequently occur in the self-consistent field (SCF).

The calculation of the f–d transitions in lanthanide phosphors is addressed with respect to the ligand field theory[13,14] but not restricted to its classical empirical frame.[15] The model Hamiltonian is parameterized in terms of a few quantities such as the Slater–Condon parameters, the spin–orbit coupling constants and the ligand field potential. The Slater–Condon parameters represent the many electron interaction in the Hamiltonian, while the spin–orbit coupling and ligand field potential account for the one-electron part. The task of computational approach consists in the determination of these parameters in a non-empirical way.[16–20] Therefore, we do not aim in this paper to describe the electrostatic interaction part of the Hamiltonian, *i.e.* the Slater–Condon parameters relevant for the multi-electron problem, for which our theoretical model has been already improved[19] and revised[21] in previous studies. The calculation of the spin–orbit coupling is placed in the growing efforts devoted nowadays to the relativistic quantum chemistry tools.[22–25]

On the other hand, the formulation of the one-electron ligand field interaction may be partly confusing since effective two-electron components may effectively participate to the parameters. A simple representation of the ligand field interaction is obtained by the perturbation approach of the one-electron wave function of the lanthanide ion ($|l,m_l\rangle$). Within this approach the actual system of two-open-shell f and d electrons has a ligand field Hamiltonian, which is constructed

[a] *Department of Chemistry of the University of Fribourg, Chemin du Musée 9, 1700 Fribourg, Switzerland. E-mail: claude.daul@unifr.ch; Fax: +41 26 300 9738; Tel: +41 26 300 8700*
[b] *Institut für Anorganische Chemie der Universität Hannover, Callinstr. 9, D-30167 Hannover, Germany. E-mail: wurland@arcor.de*
[c] *Institute of Physical Chemistry, Splaiul Independentei 202, Bucharest 060021, Romania. E-mail: cfanica@yahoo.com*

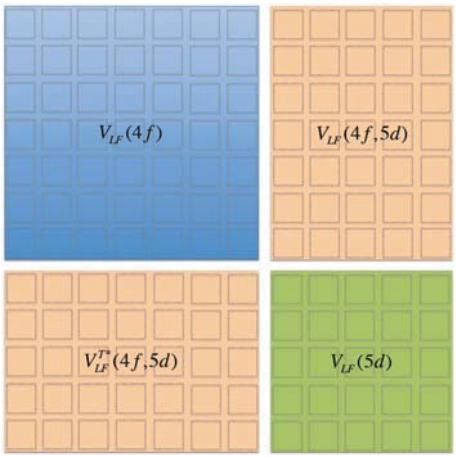

Fig. 1 Schematic representation of the ligand field matrix V_{LF} corresponding to the merged 4f and 5d orbitals in the problem of two-open-shell 4f and 5d electrons.

on the basis of the merged 4f (l = 3) and 5d (l = 2) orbitals of the lanthanide ion, *i.e.* seven plus five $|l,m_l\rangle$ functions (see Fig. 1).

Dorenbos[26] has taken the relative simplicity of this representation (Fig. 1), and the related eigenvalues, to create a model widely applied in some empirical-to-semi-empirical studies. One can recognize from Fig. 1 the shape of the actual ligand field Hamiltonian, where diagonal sub-blocks of 7 by 7 ($V_{LF}(4f)$) and 5 by 5 elements ($V_{LF}(5d)$) are a direct perturbation of the 4f and 5d orbitals of the lanthanide ion. An off-diagonal sub-block of 7 by 5 elements is also present. This $V_{LF}(4f,5d)$ block matrix is a perturbation in a second order, whose presence is governed by basic group theory rules, *i.e.* $V_{LF}(4f,5d)$ vanishes if the local symmetry of the lanthanide coordination exhibits inversion center. Without going into details since the theory has been already described in different textbooks,[27,28] Wybourne has defined the ligand field potential as a linear combination of spherical harmonics $Y_{k,q}$ up to a given order. Accordingly, a general expansion expression of each sub-block in Fig. 1 is presented in eqn (1):

$$V_{LF}(4f) = \sum_{k=0,2,4,6} \sum_{q=-k}^{k} B_q^k(4f) C_q^{(k)}, \quad (1a)$$

$$V_{LF}(5d) = \sum_{k=0,2,4} \sum_{q=-k}^{k} B_q^k(5d) C_q^{(k)}, \quad (1b)$$

$$V_{LF}(4f,5d) = \sum_{k=1,3,5} \sum_{q=-k}^{k} B_q^k(4f,5d) C_q^{(k)}, \quad (1c)$$

where $C_q^{(k)}$ are the solid spherical harmonic tensor operators (eqn (2)) and B_q^k's are the Wybourne-normalized crystal field parameters:

$$C_q^{(k)} = \sqrt{\frac{4\pi}{2k+1}} Y_{k,q} \quad (2)$$

Analogous representations related by simple convention factors with the above formalism also exist *e.g.* following the definition of $A_{k,q}$'s given by Stevens[27,29] for instance. However the main idea of the representation in eqn (1) is the treatment of the interaction having an electrostatic origin, avoiding any overlap between the 4f and 5d orbitals of the lanthanide ion with the ligands. Eqn (1) resemble the initial electrostatic form of crystal field theory[30] but the parameters tacitly incorporate other contributions into the metal–ligand bonding. A formal drawback of spherical Harmonics expansion is that the total Hamiltonian cannot be formulated as the sum of contributions eqn (1a) + eqn (1b) + eqn (1c) but must conceive separate operators for the 4f and 5d blocks. This is because we cannot prevent a given $C_q^{(k)}$ (with $k \leq 4$) from eqn (1a) (4f block) to interact with the spherical harmonics with appropriate symmetry originating from the 5d block. This would make the 5d ($B_q^k(5d)$) parameters identical to the $k \leq 4$ subset of the 4f ones. However this formal drawback is tacitly neglected, considering directly the parameterized blocks instead of a primordial common Hamiltonian. A part of such conceptual drawbacks is circumvented working with models explicitly based on different types of bonding effects, as is the case of the Angular Overlap Model (AOM).

In this paper, we extend the traditional concept of the AOM designed by Schäffer and Jørgensen[31] and Urland[32] for single-open-shell d and f electrons, respectively, to tackle the actual ligand field potential for two-open-shell f and d electrons necessary for the reliable understanding of the f–d transitions in lanthanide phosphors. We use the advances of our previously developed Ligand Field Density Functional Theory (LFDFT)[19] method extending it to the f–d transitions. We take the advantages given by the AOM formalism to reconsider more explicitly the ligand field interaction in the LFDFT Hamiltonian to provide general information about the chemistry of the interaction between the lanthanide ion and the ligands. This outline treatment due to AOM implies chemical intuitiveness and allows validation of the theoretical work.

Theory

In our conceptual formulation of the ligand field theory into Density Functional Theory (DFT),[16–20] LFDFT presents an effective Hamiltonian, which acts only in the subspace of the microstates originating from the ground $4f^n$ and excited $4f^{n-1}5d^1$ electron configurations of the lanthanide ion subject to perturbations due to (1) electrostatic interaction inter-electron repulsion, (2) spin–orbit coupling interaction and (3) ligand field interaction from the chemical environment. Every interaction is parameterized according to the LFDFT methodology in the way detailed in ref. 19. Considering especially the ligand field interaction, its representation as shown in eqn (1) yields 28 $B_q^k(4f)$, 15 $B_q^k(5d)$ and 21 $B_q^k(4f,5d)$ parameters (altogether, 64 parameters), where most of them may vanish due to symmetry. For instance within the octahedral ligand field, like in the case of Pr^{3+} doped into the trivalent site of the

Cs_2KYF_6 crystallizing in the elpasolite structure type,[19] the ligand field potential (eqn (1)) reduces to the following scheme (eqn (3)):

$$V_{LF}(4f) = B_0^4(4f)\left[C_0^{(4)} + \sqrt{\frac{5}{14}}\left(C_4^{(4)} + C_{-4}^{(4)}\right)\right] + B_0^6(4f)\left[C_0^{(6)} - \sqrt{\frac{7}{2}}\left(C_4^{(6)} + C_{-4}^{(6)}\right)\right] \quad (3a)$$

$$V_{LF}(5d) = B_0^4(5d)\left[C_0^{(4)} + \sqrt{\frac{5}{14}}\left(C_4^{(4)} + C_{-4}^{(4)}\right)\right] \quad (3b)$$

$$V_{LF}(4f,5d) = 0 \quad (3c)$$

In fact, only the parameters $B_0^4(4f)$, $B_0^6(4f)$ and $B_0^4(5d)$ are symmetry independent in the O_h ligand field, since $B_4^4(4f)$, $B_4^6(4f)$ and $B_4^4(5d)$ can be defined in terms of the previous ones (eqn (3)).

Because we are often confronting with low site symmetry of the lanthanide coordination obtained from the experimental synthesis of modern phosphors,[33–35] the tractability of the Wybourne-normalized crystal field parameters is cumbersome, while the AOM representation seems to be more adequate. The theory of AOM has already been described and reviewed[36] for d-[31] and f-electrons,[32] respectively. Hereafter, we are just giving a short description of the model if extended for two-open-shell f and d electrons.

In the AOM formalism, each ligand is assigned with parameters e_σ, e_π, e_δ and e_φ classified according to its overlap with the lanthanide ion to give a σ, π, δ and φ bond, respectively. In Fig. 2, we present the AOM parameters in their original definitions, *i.e.* interaction between a lanthanide ion and a ligand within $C_{\infty v}$ symmetry. Chemical bonding up to δ and φ bonds is rarely reached by the ligand orbitals, allowing us to neglect for convenience the effect of e_δ and e_φ in the representation given in Fig. 2 either for the 4f or the 5d energy splitting.

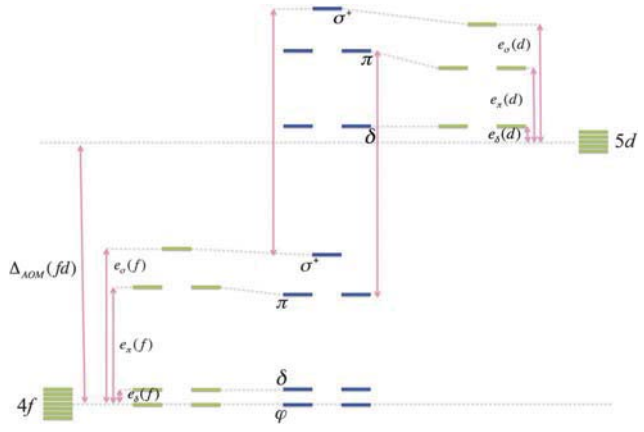

Fig. 2 Representation of the AOM parameters adjusted from the interaction of a lanthanide ion with one ligand. The first order energy splitting of the 4f and 5d orbitals is presented in green and the second order energy splitting in blue.

The definition of the parameter $\Delta_{AOM}(fd)$ (Fig. 2) is connected to the Δ(fd), which is already discussed in ref. 19 and 21. This parameter represents the energy shift of the 5d orbitals with respect to the 4f ones (Fig. 2). In cases with more than one electron it cannot be discriminated in the spectral terms from a gap due to the Slater–Condon $F_0(ff)$ and $F_0(fd)$ parameters. Thus for the Pr^{3+} complexes[19,21] taken as examples in the following, we obtain:

$$\Delta(fd) = F_0(fd) - F_0(ff) + B_0^0(5d) - B_0^0(4f) \quad (4a)$$

where, the one-electron ligand field interaction intervenes in eqn (4a) in a spherical average $B_0^0(4f)$ and $B_0^0(5d)$.

Hence the ligand field potential according to eqn (1) becomes a traceless block without Δ(fd) in line with the Wybourne formalism,[27,28] which is not the case in the formalism of AOM.[31,32] The mapping between both formalisms is obtained by adjusting the trace of the ligand field matrix obtained in the AOM with $\Delta_{AOM}(fd)$ (eqn (4b)).

$$\Delta_{AOM}(fd) = \Delta(fd) + \frac{1}{7}\mathrm{trace}(\langle 3|V_{LF}|3\rangle) - \frac{1}{5}\mathrm{trace}(\langle 2|V_{LF}|2\rangle) \quad (4b)$$

This $\Delta_{AOM}(fd)$ parameter will appear in the diagonal element of the $V_{LF}(5d)$ block matrix. Within the first order approximation for a given ligand donor, we define $e_\sigma(f)$, $e_\pi(f)$, $e_\sigma(d)$ and $e_\pi(d)$ parameters in line with the AOM formalism. Taking however the inclusion of a second order perturbation, each ligand donor obtains a novel set of AOM parameters. We define $e_\sigma(fd)$ and $e_\pi(fd)$ as is represented in Fig. 2. Anisotropy in the π interaction allows us to distinguish between $e_{\pi x}$ and $e_{\pi y}$ in the definition of the AOM parameters.[31,32] Therefore the general matrix element V_{LF} corresponding to the covalent interaction of both the 4f and 5d orbitals with the ligands is developed (eqn (5)), following the earlier approach of single-open-shell d electrons by Schäffer and Jørgensen[31] and f electrons by Urland:[32]

$$\langle 3,\mu|V_{LF}|3,\nu\rangle = \sum_{k=1}^{\text{ligands}} \sum_{\lambda=\sigma,\pi} D_{\mu\lambda}^{4f}(k)\cdot D_{\nu\lambda}^{4f}(k)\cdot e_{\lambda,k}(f) \quad (5a)$$

$$\langle 2,\mu|V_{LF}|2,\nu\rangle = \sum_{k=1}^{\text{ligands}} \sum_{\lambda=\sigma,\pi} D_{\mu\lambda}^{5d}(k)\cdot D_{\nu\lambda}^{5d}(k)\cdot e_{\lambda,k}(d) \quad (5b)$$

$$\langle 3,\mu|V_{LF}|2,\nu\rangle = \sum_{k=1}^{\text{ligands}} \sum_{\lambda=\sigma,\pi} D_{\mu\lambda}^{4f}(k)\cdot D_{\nu\lambda}^{5d}(k)\cdot e_{\lambda,k}(fd) \quad (5c)$$

where D^{4f} and D^{5d} are the matrix elements defined in terms of the Euler angles (Wigner's Darstellungsmatrizen) or direction cosines already described in ref. 31 and 32, respectively, and k is the running index for the ligand system. The eigenvalues of the V_{LF} matrix in the way it is calculated from eqn (5) can be determined analytically for the interaction between a lanthanide ion and a ligand within $C_{\infty v}$ symmetry (Fig. 2). These eigenvalues are presented in eqn (6) and (7), respectively, for the perturbation

of the 4f and 5d orbitals:

$$\langle 3,\lambda|V_{LF}|3,\lambda\rangle = \frac{1}{2}(\Delta_{AOM}(fd) + e_\lambda(d) + e_\lambda(f)) - \frac{1}{2}\sqrt{(\Delta_{AOM}(fd) + e_\lambda(d) - e_\lambda(f))^2 + 4e_\lambda{}^2(fd)} \quad (6)$$

$$\langle 2,\lambda|V_{LF}|2,\lambda\rangle = \frac{1}{2}(\Delta_{AOM}(fd) + e_\lambda(d) + e_\lambda(f)) + \frac{1}{2}\sqrt{(\Delta_{AOM}(fd) + e_\lambda(d) - e_\lambda(f))^2 + 4e_\lambda{}^2(fd)} \quad (7)$$

where, $\lambda = \sigma$, πx and πy.

One can see that the mixed parameters $e_\sigma(fd)$ and $e_\pi(fd)$ have to be small without impinging on the first order AOM parameters. The absence of them leads to the formulation of the eigenvalues (eqn (6) and (7)) in their original representations given in ref. 31 and 32, respectively. We map the ligand field matrix obtained from the LFDFT calculation with eqn (5) in order to extract AOM parameters ($e_\sigma(f)$, $e_\pi(f)$, $e_\sigma(d)$, $e_\pi(d)$, $e_\sigma(fd)$, $e_\pi(fd)$ and $\Delta_{AOM}(fd)$) in their definitions described in this section. The presented model is applied next for the calculation of the electronic structure of eightfold coordinated trivalent Pr^{3+} complexes: $(PrX_8)^{5-}$, with X = F^-, Cl^- and Br^- having an arrangement either with D_{4h} and D_{4d} symmetry, respectively.

Computational details

The DFT calculations reported in this paper have been carried out by means of the Amsterdam Density Functional (ADF2010) program package.[37–39] The local density approximation (LDA) functional based on the Vosko–Wilk–Nussair (VWN)[40] parameterization has been used for geometry consideration. The LFDFT calculation has been performed using DFT calculation based on the hybrid B3LYP functional as is implemented in the ADF program package[37–39] for the exchange and correlation energy and potential. Positive point charges are added to neutralize the highly negative charged structure using the *Efield* keyword available in the ADF program package.[37–39] The molecular orbitals were expanded using a triple-ζ STO basis set plus two polarization functions (TZ2P+) for the Pr atom and plus one polarization function (TZP) for the halogen atoms, *i.e.* F, Cl and Br. The LFDFT calculations were achieved following the detailed procedure already described in ref. 19 where the most important step consists of the representation of the density in a totally symmetric form using the approach of the Average of Calculation (AOC)[41] type calculation. The 12 by 12 ligand field matrix (in the same shape as is presented in Fig. 1) being the representative of the ligand field potential was extracted for the purpose of this work. Matlab/Octave codes for the LFDFT program together with the determination of the AOM and the Wybourne-normalized crystal field parameters from the ligand field matrix are available from the authors upon request.

The structures of the theoretical complex $(PrX_8)^{5-}$, with X = F^-, Cl^- and Br^- were obtained from the DFT geometry optimization of the cluster $(PrX_8Na_8)^{3+}$, with X = F^-, Cl^- and Br^-. The geometry of this cluster was optimized while the electronic structure was confined to have the AOC occupation of the 4f orbitals of the Pr^{3+} center and the symmetry was constrained to have the arrangement of either the D_{4h} or the D_{4d} symmetry.

Results and discussion

Pr^{3+} with eight ligands in its coordination sphere is commonly met in inorganic coordination complexes and solid state compounds. In the field of luminescent materials, Pr^{3+} has been doped into various fluoride host lattices such as $NaYF_4$,[42] CaF_2 or $LiYF_4$,[43] *etc.* resulting in eight coordination, in order to investigate the possibility of the quantum cutting process in the optical behavior.[43] If doped into the CaF_2 host lattice or the α-cubic phase of $NaYF_4$,[42] the eight coordination is typically found having a cubic arrangement (O_h point group), which might always be subjected to a slight distortion to D_{4h} symmetry. The occurrence of a D_{4d} arrangement of the eight ligands is not usual in solid state compounds, to the best of our knowledge, although it exists in inorganic coordination complexes whose properties are well recognized in the topic of magnetic anisotropy, being important in single ion magnets.[44,45] In the application of our AOM extended for two-open-shell f and d electrons, we consider here as theoretical example $(PrX_8)^{5-}$, with X = F^-, Cl^- and Br^-, having an arrangement of the D_{4h} or the D_{4d} point group, insofar as the eight ligands are identical and equivalent by symmetry (Fig. 3).

The structures of the eightfold coordinated Pr^{3+} are calculated while the optimization of the geometry is confined within the desired symmetry, *i.e.* dependent on a few parameters such as the Pr^{3+}–ligand bond length d and the polar angle θ in spherical coordinates. The azimuthal angle ϕ is fixed for each of the eight ligands in the arrangement with either D_{4h} or D_{4d} symmetry. We present in Table 1 these spherical coordinates deduced from the optimized structures. The optimized structures in question are calculated as clusters, being representative only in semiquantitative sense, since the full lattice effects are idealized by compensating charges. Accordingly, the theoretical structures (Table 1) might not represent a global minimum of

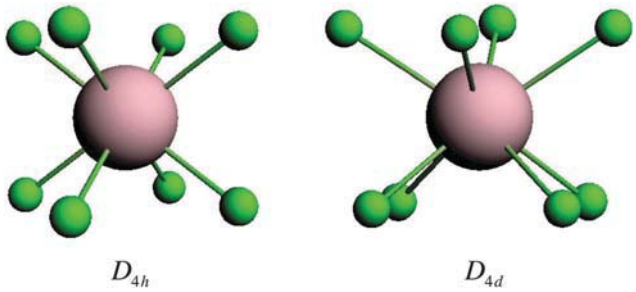

Fig. 3 Spatial representations of the structure of $(PrX_8)^{5-}$ (X = F^-, Cl^-, Br^-) with D_{4h} (left hand side) and D_{4d} (right hand side) arrangements.

Table 1 DFT calculated geometries of $(PrX_8)^{5-}$ (X = F^-, Cl^-, Br^-): Pr^{3+}–X bond length d in Å and the polar coordinate θ in ° of one ligand X from which the rest of the ligand coordinates is generated by symmetry

	D_{4h}		D_{4d}	
	d	θ	d	θ
$(PrF_8)^{5-}$	2.372	54.75	2.368	56.95
$(PrCl_8)^{5-}$	2.853	54.78	2.825	57.91
$(PrBr_8)^{5-}$	3.007	54.74	2.973	58.34

the energy in the adiabatic potential energy surface validated by frequency analysis of all the normal modes.

The optimization of the geometry, if confined to the D_{4h} symmetry under the present computational details, leads to a nearly cubic arrangement (O_h point group) of the eight ligands (Table 1). The bond lengths determined for both structures having D_{4h} and D_{4d} symmetry (Table 1) are in agreement with the Shannon radii[46] of Pr^{3+} and the ligand ions in such an eight coordination. The D_{4h} ligand field splits the 4f and 5d orbitals of Pr^{3+} into a_{2u}, b_{1u}, b_{2u}, $2e_u$ and a_{1g}, b_{1g}, b_{2g}, e_g (*cf.* Fig. 4), respectively, representative of the irreducible representations (*irreps*) of the D_{4h} point group. These representations can be separately discriminated using the inversion center symmetry operator since the 4f and 5d possess opposite parity in D_{4h}. This particular situation allows no mixing of the two-open-shell

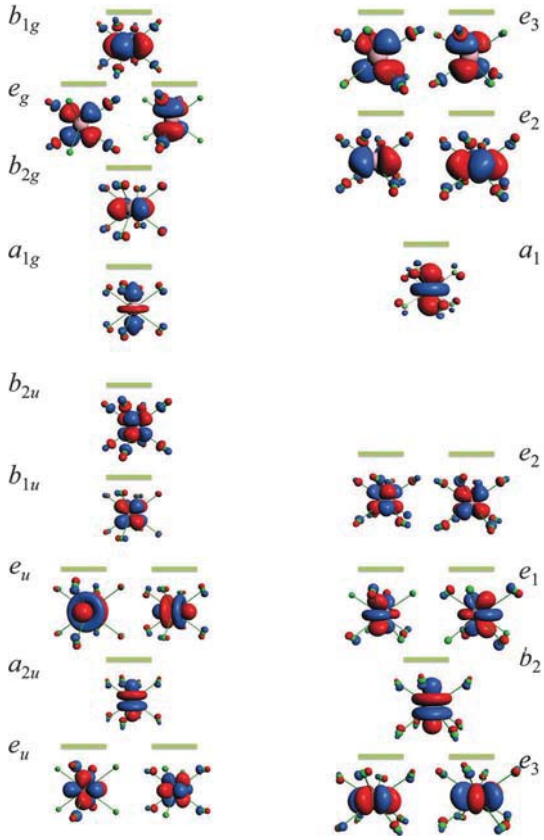

Fig. 4 Splitting pattern of the seven 4f and five 5d orbitals of Pr^{3+} in the presence of a ligand field of D_{4h} (left hand side) and D_{4d} (right hand side) symmetry.

4f and 5d electrons in the investigation of the $4f^15d^1$ electron configuration of Pr^{3+}, *i.e.* the $V_{LF}(4f,5d)$ block matrix has strictly zero elements. On the other hand, the D_{4d} ligand field splits the 4f and 5d orbitals into b_2, e_1, e_2, e_3 and a_1, e_2, e_3 *irreps* (*cf.* Fig. 4), respectively. It is obviously seen that the e_2 as well as the e_3 *irreps* allow mixing of some 4f and 5d $|l,m_l\rangle$ functions. This situation therefore leads us to consider more explicitly the off-diagonal elements of the V_{LF} matrix, being parameterized by the mixed AOM $e_\sigma(fd)$ and $e_\pi(fd)$ parameters.

There are other circumstances under which the elements of the $V_{LF}(4f,5d)$ block matrix may be significant, being therefore important in the analysis of the luminescence of lanthanide phosphors. So for example when Pr^{3+} is doped into $Y_3Al_5O_{12}$ (ref. 15) or $LiYF_4$ (ref. 43, 47 and 48) having a local symmetry of D_{2d} and S_4, respectively, or the frequently occurred C_1 ligand field in YF_3:Pr^{3+},[49,50] for instance.

The AOM extended for two-open-shell f and d electrons provides: both a perturbation correction of the ligand field potential for the 4f and 5d open shells, and an additional mechanism that has to affect the multiplet energy levels and more importantly their intensities. A graphical representation of the energy splitting pattern of the 4f and 5d orbitals of Pr^{3+} together with the molecular orbital diagram is shown in Fig. 4 considering the $4f^15d^1$ electron configuration, in both arrangements of D_{4h} and D_{4d} symmetry, respectively.

Taking the structures given in Table 1 as input, we perform the LFDFT calculation and extract the ligand field potential on which we focus our interest. The Slater–Condon parameters are also obtained from the LFDFT calculation and presented in Table 2.

We use the procedure as is described in ref. 21, using the radial functions of the 4f and 5d Kohn–Sham orbitals of Pr^{3+} to extract the Slater–Condon parameters. These radial functions are graphically presented in Fig. 5 considering the free Pr^{3+} ion and its complex with eight fluoride, chloride and bromide ligands forming a D_{4h} arrangement. Since the Slater–Condon parameters are not treated prior to the ligand field potential in this paper, we present them in Table 2 as average between the quantities obtained for the D_{4h} and D_{4d} arrangements of $(PrX_8)^{5-}$, with X = F^-, Cl^-, Br^-. It is noteworthy that the parameters (Table 2) are not strongly sensitive to the change of the spatial arrangement of the eight ligands around Pr^{3+}. The quantities given in Table 2 are in the magnitude of known experimental fitted parameters.[51] The Slater–Condon parameters $G_1(fd)$, $F_2(fd)$, $G_3(fd)$, $F_4(fd)$, and $G_5(fd)$ appropriate to

Table 2 LFDFT calculated Slater–Condon parameters in cm^{-1} obtained for the system $(PrX_8)^{5-}$, with X = F^-, Cl^-, Br^-

	$(PrF_8)^{5-}$	$(PrCl_8)^{5-}$	$(PrBr_8)^{5-}$
$F_2(ff)$	330.0	323.1	322.1
$F_4(ff)$	43.0	41.9	41.8
$F_6(ff)$	4.6	4.5	4.4
$G_1(fd)$	296.3	227.5	179.8
$F_2(fd)$	210.7	144.3	117.5
$G_3(fd)$	26.7	18.5	14.5
$F_4(fd)$	16.0	10.5	8.3
$G_5(fd)$	4.2	2.8	2.2

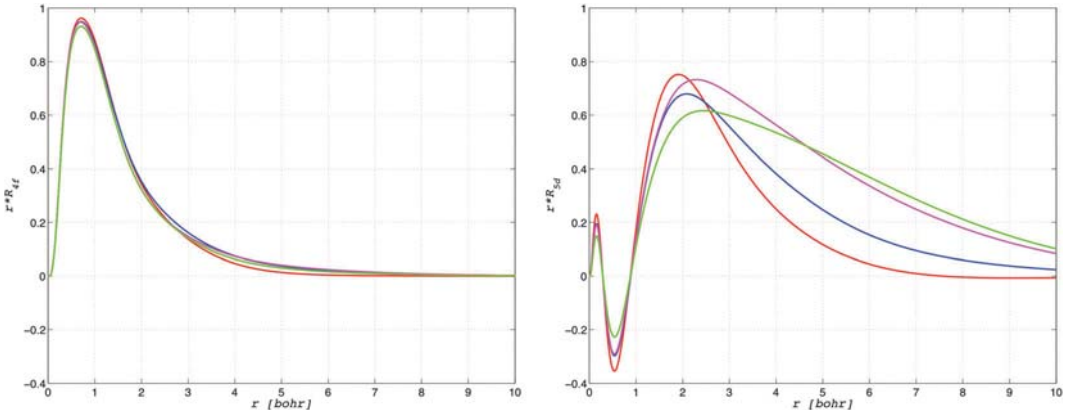

Fig. 5 Graphical representation of the radial functions of the 4f (left hand side) and 5d (right hand side) Kohn–Sham orbitals of the free Pr^{3+} ion (in red) and the complexes $(PrF_8)^{5-}$ (in blue), $(PrCl_8)^{5-}$ (in magenta) and $(PrBr_8)^{5-}$ (in green), forming a D_{4h} arrangement.

the splitting of terms sharing the $4f^15d^1$ electron configuration parentage diminish in the series F^-, Cl^- and Br^- ligands, in line with the increasing of the nephelauxetic effect obtained for the same series of ligands. The nephelauxetic effect denominates an expansion of the electron cloud as is presented in Fig. 5. The radial function of the 5d Kohn–Sham orbital, but also the 4f one although the effect is weaker, is expanded toward the ligands. This expansion is weak in the case of the 5d in $(PrF_8)^{5-}$ but becomes stronger for chloride and bromide systems. However in the same series of ligands, the F_2(ff), F_4(ff), and F_6(ff) parameters ($4f^2$ electron configuration) are almost invariant showing the relative shielding of the 4f orbitals by the outer shells in contrast to the 5d ones (*cf.* Fig. 5). The spin–orbit coupling constants ζ_{4f} and ζ_{5d} are also calculated using the approach of ZORA relativistic available in the ADF program package,[37–39] where we obtain (in cm^{-1}) 760 and 945, respectively.

The AOM parameters are calculated by mapping the matrix elements of V_{LF} given by eqn (5) to the ligand field potential obtained by the LFDFT procedure. These quantities are presented in Table 3, where only one set of the AOM parameters appears since the eight ligands are identical and equivalent by symmetry in the structures being investigated. Although the Pr^{3+}–ligand bond lengths obtained in the DFT optimization of the D_{4h} structures are slightly elongated if compared to the D_{4d} ones (*cf.* Table 1), we expect no significant changes in the AOM parameters as depicted in Table 3. The difference between the D_{4h} and D_{4d} ligand field potentials is essentially made by the mixed AOM parameters e_σ(fd) and e_π(fd) in the V_{LF}(4f,5d) block matrix elements.

Table 3 DFT calculated AOM parameters in cm^{-1} for the ligand field potential of $(PrX_8)^{5-}$ (X = F^-, Cl^-, Br^-) with arrangement in D_{4h} and D_{4d} symmetry

	D_{4h}			D_{4d}		
	$(PrF_8)^{5-}$	$(PrCl_8)^{5-}$	$(PrBr_8)^{5-}$	$(PrF_8)^{5-}$	$(PrCl_8)^{5-}$	$(PrBr_8)^{5-}$
e_σ(f)	534	214	105	417	186	101
e_π(f)	71	88	34	194	84	45
e_σ(d)	13 040	4536	3997	13 091	4558	3965
e_π(d)	3732	2405	2365	2341	2365	2514
e_σ(fd)	0	0	0	3456	429	248
e_π(fd)	0	0	0	2179	257	123
Δ_{AOM}(fd)	19 351	16 741	11 339	22 075	17 397	11 755

The strength of the ligand field is directly related to the AOM parameters (Table 3), where the fluoride ligands exert the largest energy splitting of both the 4f and 5d orbitals. This is perfectly in line with the spectrochemical series for ligands. The definition of the novel mixed parameters e_σ(fd) and e_π(fd) in the present theoretical section leads to quantities which are lying between the e_σ(f), e_σ(d), and e_π(f), e_π(d), respectively, as shown in Table 3. Although in this paper we address theoretical examples based on Pr–halides complexes, the AOM parameters have the recognized advantages to be transferable giving further insight into their comparison to available experimental deduced parameters. Urland[52] experimentally deduced e_σ(f) = 552 cm^{-1} in the system $LiYF_4$:Pr^{3+} (eightfold coordinate $(PrF_8)^{5-}$ having S_4 arrangement)[52] with a ratio $e_\sigma(f)/e_\pi(f)$ = 5.34, in the magnitude of our calculated parameters (Table 3). For a chloride system, e_σ(f) = 235 cm^{-1} was deduced experimentally in Pr^{3+}-doped $LaCl_3$,[53] also in line with the calculated parameters given in Table 3. Experimentally deduced Wybourne-normalized crystal field parameters for bromide systems (Pr^{3+}-doped $ThBr_4$) are also available in ref. 54, which indicate *a priori* AOM parameters in the magnitude of Table 3, providing validation of the calculated parameters.

We carried out the investigation by focusing more deeply on the D_{4d} ligand field, for which the presence of the mixed AOM parameters is attested. To obtain the eigenvalues of the V_{LF} matrix in their representation given in Fig. 4, we calculate analytically the V_{LF} matrix elements for the case of the D_{4d} ligand field. The given analytical expressions are rigorously adequate for any practical example since we present them also in terms of the polar angle θ (*cf.* Table 1), the AOM parameters containing by definition information about the metal–ligand bond length.[31,32] In the D_{4d} ligand field, the split of the 4f orbitals in the b_2, e_1, e_2, e_3 *irreps* follows the classification of ml = {0, ±1, ±2, ±3} components. In the same way, the split of the 5d in the a_1, e_2, e_3 *irreps* gets ml = {0, ± 2, ± 1}. Within the

first order perturbation, most elements of the V_{LF} matrix are zero, the non-vanishing elements remaining only in the diagonal as given in eqn (8) and (9):

$$\langle 3,b_2|V_{LF}|3,b_2\rangle = 2e_\sigma(f)\left(5\cos^3\theta - 3\cos\theta\right)^2 + 3e_\pi(f)\left(4\sin\theta - 5\sin^3\theta\right)^2 \quad (8a)$$

$$\langle 3,e_1|V_{LF}|3,e_1\rangle = \frac{3}{2}e_\sigma(f)\left(4\sin\theta - 5\sin^3\theta\right)^2 + \frac{1}{4}e_\pi(f)\left(225\cos^6\theta - 305\cos^4\theta + 111\cos^2\theta + 1\right) \quad (8b)$$

$$\langle 3,e_2|V_{LF}|3,e_2\rangle = 15e_\sigma(f)\left(\cos\theta - \cos^3\theta\right)^2 + 10e_\pi(f)\left(\frac{9}{4}\sin^6\theta - 4\sin^4\theta + 2\sin^2\theta\right) \quad (8c)$$

$$\langle 3,e_3|V_{LF}|3,e_3\rangle = \frac{5}{2}e_\sigma(f)\sin^6\theta + \frac{15}{4}e_\pi(f)\left(\sin^4\theta + \left(\cos\theta - \cos^3\theta\right)^2\right) \quad (8d)$$

$$\langle 2,a_1|V_{LF}|2,a_1\rangle = \Delta_{AOM}(fd) + 2e_\sigma(d)\left(3\sin^2\theta - 2\right)^2 + 24e_\pi(d)\cos^2\theta\sin^2\theta \quad (9a)$$

$$\langle 2,e_2|V_{LF}|2,e_2\rangle = \Delta_{AOM}(fd) + 12e_\sigma(d)\cos^2\theta\sin^2\theta + 4e_\pi(d)\left(4\cos^4\theta - 3\cos^2\theta + 1\right) \quad (9b)$$

$$\langle 2,e_3|V_{LF}|2,e_3\rangle = \Delta_{AOM}(fd) + 3e_\sigma(d)\sin^4\theta + 4e_\pi(d)\sin^2\theta\left(1 + \cos^2\theta\right) \quad (9c)$$

Furthermore, within the second order perturbation, the e_2 and e_3 *irreps*, being present in the transformation of both f and d, allow mixing of the 4f and 5d functions as stated earlier, leading to the formation of off-diagonal elements located in the V_{LF}(4f,5d) block matrix (eqn (10)):

$$\langle 3,e_2|V_{LF}|2,e_2\rangle = \sqrt{30}\cos\theta\sin^4\theta\left(e_\sigma(fd) - \sqrt{2}e_\pi(fd)\right) \quad (10a)$$

$$\langle 3,e_3|V_{LF}|2,e_3\rangle = 3\sqrt{5}\cos\theta\sin^4\theta\left(e_\sigma(fd) - \sqrt{2}e_\pi(fd)\right) \quad (10b)$$

To ensure the double degeneracy of the e_1, e_2 and e_3 *irreps*, the matrix elements given in eqn (8b)–(8d), (9b), (9c), (10a) and (10b) are always multiplied by an identity matrix of dimension 2.

Amongst the thirty-five elements of the V_{LF}(4f,5d) block matrix, four elements are non-zero in the D_{4d} ligand field, which are two by two equivalents as shown in eqn (10). Although the e_2 and e_3 *irreps* are well distinguished in the D_{4d} point group, the AOM formalism up to second order does not differentiate them in the perturbation considering the isotropic π-interaction of the Pr^{3+}–ligand bond. Indeed eqn (10a) can be obtained from eqn (10b) by multiplying it with a factor of $\sqrt{6}/3$. Therefore the slight stabilization of the eigenvalue of the $|3,e_2\rangle$ function due to the presence of the off-diagonal elements in the V_{LF} matrix (eqn (10)), which is equal to the destabilization of the eigenvalue of the $|2,e_2\rangle$ function, is connected to the energy stabilization of the$|3,e_3\rangle$, which is also equivalent to the destabilization of the $|2,e_3\rangle$, weighted with a constant factor. This factor is not in reality fixed as we obtain from the non-empirical DFT calculation. It can be definitely dismissed in the AOM considering the formulation of two different e_π(fd) parameters such as $e_{\pi x}$(fd) and $e_{\pi y}$(fd), respectively. These two parameters, while different, will conserve an intrinsic degeneracy of either e_2 or e_3 *irrep* in the D_{4d} point group. This is intriguing but without any doubt in the definition of the second order AOM perturbation. Hence we present in Table 3 one of those e_π(fd) parameters since the another one is set to zero in the mapping of AOM to the DFT results (eqn (5)). It is noteworthy to emphasize that the exact consideration of the AOM for two-open-shell f and d electrons requires too many parameters, which by convenience we enforce to fit with only seven parameters (e_σ(f), e_π(f), e_σ(d), e_π(d), e_σ(fd), e_π(fd), Δ_{AOM}(fd)). The non-considered parameters do not vanish but their influence is subtly engulfed into the active list in Table 3, the V_{LF} matrix from eqn (5) being as accurate as the calculated non-empirical DFT one.

Since most of the theoretical and experimental studies are adopting the Wybourne-normalized crystal field formalism,[47,48,50,55–58] we present for comparison by means of eqn (11) the B_q^k's values (eqn (1)) obtained from the computed matrix elements of V_{LF} (see eqn (5)):

$$\langle l,m_l|V_{LF}|l',m_{l'}\rangle = \sum_k\sum_{q=-k}^{k} B_q^k(l,l')\langle l,m_l|C_q^{(k)}|l',m_{l'}\rangle \quad (11)$$

where $\langle l,m_l|C_q^{(k)}|l',m_{l'}\rangle$ is a coupling coefficient.

The B_q^k's are presented in Table 4 for the comparison purpose considering the eightfold complexes of Pr^{3+} ions under consideration. In total this formalism requires ten parameters in the actual problem of the D_{4d} ligand field, which is by far superseded by our seven parameters obtained from the AOM formalism.

Table 4 DFT calculated Wybourne-normalized crystal field parameters in cm^{-1} for the ligand field potential of $(PrX_8)^{5-}$ (X = F^-, Cl^-, Br^-) with D_{4h} and D_{4d} symmetry

	D_{4h}			D_{4d}		
	$(PrF_8)^{5-}$	$(PrCl_8)^{5-}$	$(PrBr_8)^{5-}$	$(PrF_8)^{5-}$	$(PrCl_8)^{5-}$	$(PrBr_8)^{5-}$
B_0^2(4f)	−3	−3	0	−346	−217	−133
B_0^4(4f)	−2634	−1148	−550	−2068	−871	−459
B_4^4(4f)	1577	689	329	0	0	0
B_0^6(4f)	1391	268	175	511	260	148
B_4^6(4f)	2595	498	328	0	0	0
Δ(fd)	51 285	31 249	25 104	49 592	31 853	25 926
B_0^2(5d)	−82	−79	1	−8929	−5697	−6059
B_0^4(5d)	−45 129	−7433	−4725	−50 719	−6773	−2875
B_4^4(5d)	27 012	4458	2823	0	0	0
B_0^1(4f,5d)	0	0	0	−5399	−835	−700
B_0^3(4f,5d)	0	0	0	6380	861	580
B_0^5(4f,5d)	0	0	0	1613	366	441

Another utility of the two-open-shell approach, which however will be not detailed here, is curing the so-called holohedrization effect[59] that leads to an artificial increase in symmetry, if traditional single-open-shell ligand field theories are used. Namely, with respect to an inversion center, the d or f block Hamiltonians can include only terms with even parity, because the matrix elements are carrying the respective g × g = g or u × u = g products. This means that an asymmetric coordination sphere is accounted non-realistically. For instance, for the case of a single metal–ligand couple, M–L, the ligand field problem in the d or f basis looks like that the perturbation is smeared in equivalent halves (L/2) on both directions of the coordination, as the ligand field is produced by a *trans*-(L/2)–M–(L/2) arrangement.

Or, in the same line of reasoning a *cis*-MX_3 pyramid with X–M–X only at 90° angles will have the same f or d splitting as an octahedron, since each ligand has distributed its perturbation in the *trans* direction too, resulting in an artificial $M(X/2)_6$. Such a *cis*-MX_3 does not exist in reality, but is a convincing thought experiment about the limitation of the classical single-open-shell ligand field Hamiltonian phenomenology. The two-open-shell approach allows the insertion of asymmetric terms, by the g × u = u parity of the f × d nondiagonal block. In this way the ligand field treatment is enhanced to more realism. Another outlook of this approach, which also is too large in technical display, being presented now only as seed idea, is that the explicit use of two-electron f–d terms may replace the use of empirical corrections, such as trees[60] or Marvin terms,[61] for amending the implication of many body effect in the ligand field Hamiltonian parameterization. The AOM extended for two-open-shell 4f and 5d electrons will therefore provide a useful tool ensuring chemical intuitiveness in the currently popular magnetic property design of lanthanide single ion magnets.[62–65]

Conclusions

Theoretical modeling is a valuable tool for the understanding of the chemical and the physical properties of molecular, coordination chemistry complexes and solid state compounds. Here we address a practical problem encountered in the non-empirical determination of the $4f^n \rightarrow 4f^{n-1}5d^1$ transitions: the ligand field interaction. We underline the need for a ligand field potential for two-open-shell 4f and 5d electrons, which is important in the formulation of a new generation of theoretical and application problems in lanthanide physical chemistry. As practical use, the two-open-shell model is of interest for the design and characterization of modern luminescent materials, aiming to provide us hopefully soon with warm-white LED lighting.

We revisit the old concept of the Angular Overlap Model (AOM), originally designed to describe the electronic structures of single-open-shell d or f electrons, to parameterize the ligand field potential obtained not only from the LFDFT calculation but also from any available computational setting which may deal with the problem. The combination of the AOM along with modern quantum chemistry tools enhances the understanding of the chemistry of lanthanides. We define new mixed AOM parameters acting in non-diagonal blocks of the two-open-shell ligand field matrix. The presented model is also appropriate for the calculation of line intensities, where the mixing of both the 4f and 5d wave functions is important. The AOM can be used to parameterize the ligand field potential for two-open-shell f and d electrons, especially in the case of low symmetry lanthanide coordination. The AOM parameters are transferable, comparable, and offer chemical insight. In low symmetry environments, the number of AOM parameters is usually smaller than those of the Wybourne-normalized crystal field schemes, a fact that enhances the transparency of the modelling. The given model contributes to the understanding of lanthanides in phosphors and presents a non-empirical approach using a less sophisticated computational procedure for the rather complex problem of ligand field of both 4f and 5d open shells.

Acknowledgements

This work is supported by the Swiss National Science Foundation (SNF) and the Swiss State Secretariat for Innovation and Research. Support from the UEFISCCDI (Romania) research grant PCE 14/2013 is also acknowledged.

Notes and references

1 S. Nakamura and G. Fasol, *The blue Laser Diode*, Springer, Berlin, 1997.
2 M. Krings, G. Montana, R. Dronskowski and C. Wickleder, *Chem. Mater.*, 2011, **23**, 1694–1699.
3 T. Jüstel, H. Nikol and C. Ronda, *Angew. Chem., Int. Ed.*, 1998, **37**, 3084–3103.
4 C. Feldmann, T. Jüstel, C. Ronda and P. J. Schmidt, *Adv. Funct. Mater.*, 2003, **13**, 511–516.
5 T. Aitasalo, J. Hassinen, J. Hölsä, T. Laamanen, M. Lastusaari, M. Malkamäki, J. Nittykoski and P. Novak, *J. Rare Earths*, 2009, **27**, 529–538.
6 M. Laroche, J.-L. Doualan, S. Girard, J. Margerie and R. Moncorgé, *J. Opt. Soc. Am. B*, 2000, **17**, 1291–1303.
7 L. van Pietersen, M. F. Reid, R. T. Wegh, S. Soverna and A. Meijerink, *Phys. Rev. B: Condens. Matter Mater. Phys.*, 2002, **65**, 045113.
8 P. S. Peijzel, P. Vergeer, A. Meijerink, M. F. Reid, L. A. Boatner and G. W. Burdick, *Phys. Rev. B: Condens. Matter Mater. Phys.*, 2005, **71**, 045116.
9 F. Cimpoesu, F. Dahan, S. Ladeira, M. Ferbinteanu and J.-P. Costes, *Inorg. Chem.*, 2012, **51**, 11279–11293.
10 J. Paulovic, F. Cimpoesu, M. Ferbinteanu and K. Hirao, *J. Am. Chem. Soc.*, 2004, **126**, 3321–3331.
11 M. Ferbinteanu, T. Kajiwara, K.-Y. Choi, H. Nojiri, A. Nakamoto, N. Kojima, F. Cimpoesu, Y. Fujimura, S. Takaishi and M. Yamashita, *J. Am. Chem. Soc.*, 2006, **128**, 9008–9009.
12 S. Tanase, M. Ferbinteanu and F. Cimpoesu, *Inorg. Chem.*, 2011, **50**, 9678–9687.
13 J. S. Griffith, *The theory of Transition Metal Ions*, Cambridge University Press, Cambridge, 1961.
14 B. N. Figgis and M. A. Hitchman, *Ligand Field theory and its application*, Wiley-VCH, New York, 2000.

15 M. D. Faucher and H. J. Kooy, *Solid State Commun.*, 1997, **102**, 663–667.
16 M. Atanasov, C. Daul and C. Rauzy, *Struct. Bonding*, 2004, **106**, 97–125.
17 F. Senn, L. Helm, A. Borel and C. A. Daul, *C. R. Chim.*, 2012, **15**, 250–254.
18 M. Atanasov, E. J. Baerends, P. Baettig, R. Bruyndonckx, C. Daul and C. Rauzy, *Chem. Phys. Lett.*, 2004, **399**, 433–439.
19 H. Ramanantoanina, W. Urland, F. Cimpoesu and C. Daul, *Phys. Chem. Chem. Phys.*, 2013, **15**, 13902–13910.
20 H. Ramanantoanina, W. Urland, A. Garcia-Fuente, F. Cimpoesu and C. Daul, *Chem. Phys. Lett.*, 2013, **588**, 260–266.
21 H. Ramanantoanina, W. Urland, A. Garcia-Fuente, F. Cimpoesu and C. Daul, *Phys. Chem. Chem. Phys.*, 2013, submitted.
22 E. van Lenthe, J. G. Snijders and E. J. Baerends, *J. Chem. Phys.*, 1996, **105**, 6505–6516.
23 J. Autschbach and T. Ziegler, *J. Chem. Phys.*, 2000, **113**, 9410–9418.
24 F. Neese, *J. Chem. Phys.*, 2005, **122**, 034107.
25 M. Atanasov, C. Rauzy, P. Baettig and C. Daul, *Int. J. Quantum Chem.*, 2004, **102**, 119–131.
26 E. G. Rogers and P. Dorenbos, *J. Lumin.*, 2014, **146**, 445–449.
27 S. Hüfner, *Optical spectra of transparent rare earth compounds*, Academic Press, New York, 1978.
28 R. D. Cowan, *The theory of atomic structure and spectra*, University of California Press, Berkeley, 1997.
29 K. H. W. Stevens, *Proc. Phys. Soc., London, Sect. A*, 1952, **65**, 209–215.
30 C. J. Ballhausen, *J. Chem. Educ.*, 1979, **56**, 215–218.
31 C. Schäffer and C. Jørgensen, *Mol. Phys.*, 1965, **9**, 401–412.
32 W. Urland, *Chem. Phys.*, 1976, **14**, 393–401.
33 M. M. Lezhnina, T. Jüstel, H. Kätker, D. U. Wiechert and U. H. Kynast, *Adv. Funct. Mater.*, 2006, **16**, 935–942.
34 E. van der Kolk, P. Dorenbos and C. W. E. van Eijk, *Opt. Commun.*, 2001, **197**, 317–326.
35 S. Kück, I. Sokolska, M. Henke, M. Döring and T. Scheffler, *J. Lumin.*, 2003, **102–103**, 176–181.
36 E. Larsen and G. N. La Mar, *J. Chem. Educ.*, 1974, **51**, 633–640.
37 G. te Velde, F. M. Bickelhaupt, S. J. A. van Gisbergen, C. F. Guerra, E. J. Baerends, J. G. Snijders and T. Ziegler, *J. Comput. Chem.*, 2001, **22**, 931–967.
38 C. F. Guerra, J. G. Snijders, G. te Velde and E. J. Baerends, *Theor. Chem. Acc.*, 1998, **99**, 391–403.
39 E. J. Baerends, T. Ziegler, J. Autschbach, D. Bashford, A. Berces, F. M. Bickelhaupt, C. Bo, P. M. Boerrigter, L. Cavallo, D. P. Chong, L. Deng, R. M. Dickson, D. E. Ellis, M. van Faassen, L. Fan, T. H. Fischer, C. F. Guerra, A. Ghysels, A. Giammona, S. J. A. van Gisbergen, A. W. Götz, J. A. Groeneveld, O. V. Gritsenko, M. Grüning, S. Gusarov, F. E. Harris, P. van den Hoek, C. R. Jacob, H. Jacobsen, L. Jensen, J. W. Kaminski, G. van Kessel, F. Koostra, A. Kovalenko, M. V. Krykunov, E. van Lenthe, D. A. McCormack, A. Michalak, M. Mitoraj, J. Neugebauer, V. P. Nicu, L. Noodleman, V. P. Osinga, S. Patchkovskii, P. H. T. Philipsen, D. Post, C. C. Pye, W. Ravenek, J. I. Rodriguez, P. Ros, P. R. T. Shipper, G. Schreckenbach, J. S. Seldenthuis, M. Seth, J. G. Snijders, M. Sola, M. Swart, D. Swerhone, G. te Velde, P. Vernooijs, L. Versluis, L. Vissher, O. Visser, F. Wang, T. Wesolowski, E. M. van Wezenbeek, G. Wiesenekker, S. K. Wolff, T. K. Woo and A. L. Yarkolev, *ADF2010.01*, available at http://www.scm.com.
40 S. Vosko, L. Wilk and M. Nussair, *Can. J. Phys.*, 1980, **58**, 1200–1211.
41 C. Daul, *Int. J. Quantum Chem.*, 1994, **52**, 867–877.
42 B. Herden, J. Nordmann, R. Komban, M. Haase and T. Jüstel, *Opt. Mater.*, 2013, **35**, 2062–2067.
43 Q. Y. Zhang and X. Y. Huang, *Prog. Mater. Sci.*, 2010, **55**, 353–427.
44 S.-D. Jiang, B.-W. Wang, G. Su, Z.-M. Wang and F. Gao, *Angew. Chem., Int. Ed.*, 2010, **122**, 7610–7613.
45 S. Takamatsu, T. Ishikawa, S.-Y. Koshihara and N. Ishikawa, *Inorg. Chem.*, 2007, **46**, 7250–7252.
46 R. D. Shannon, *Acta Crystallogr., Sect. A: Cryst. Phys., Diffr., Theor. Gen. Crystallogr.*, 1976, **32**, 751–767.
47 M. F. Reid, L. van Pieterson, R. T. Wegh and A. Meijerink, *Phys. Rev. B: Condens. Matter Mater. Phys.*, 2000, **62**, 14744–14749.
48 D. Wang, S. Huang, F. You, S. Qi, Y. Fu, G. Zhang, J. Xu and Y. Huang, *J. Lumin.*, 2007, **122–123**, 450–452.
49 J. K. Sommerdijk, A. Bril and W. de Jager, *J. Lumin.*, 1974, **8**, 341–343.
50 W. Piper, J. A. DeLuca and F. S. Ham, *J. Lumin.*, 1974, **8**, 344–348.
51 G. W. Burdick and M. F. Reid, *Handb. Phys. Chem. Rare Earths*, 2007, **37**, 61–98.
52 W. Urland, *Chem. Phys. Lett.*, 1981, **77**, 58–62.
53 A. Bencini, C. Beneli and D. Gatteschi, *Coord. Chem. Rev.*, 1984, **60**, 131–169.
54 J. G. Conway, J. C. Krupa, P. Delamoye and M. Genet, *J. Chem. Phys.*, 1981, **74**, 849–852.
55 M. D. Faucher and O. K. Moune, *Phys. Rev. A: At., Mol., Opt. Phys.*, 1997, **55**, 4150–4154.
56 C.-K. Duan, P. A. Tanner, V. Makhov and N. Khaidukov, *J. Phys. Chem. A*, 2011, **115**, 8870–8876.
57 W. W. Lukens, N. M. Edelstein, N. Magnani, T. W. Hayton, S. Fortier and L. A. Seaman, *J. Am. Chem. Soc.*, 2013, **135**, 10742–10754.
58 P. A. Tanner, C. S. K. Mak, M. D. Faucher, W. M. Kwok, D. L. Philips and V. Mikhailik, *Phys. Rev. B: Condens. Matter Mater. Phys.*, 2003, **67**, 115102.
59 C. F. Schäffer, *Proc. R. Soc. London, Ser. A*, 1967, **297**, 96–133.
60 B. R. Judd, *J. Chem. Phys.*, 1966, **44**, 839–840.
61 H. H. Marvin, *Phys. Rev.*, 1947, **71**, 102–110.
62 N. F. Chilton, D. Collison, E. J. L. McInnes, R. E. P. Winpenny and A. Soncini, *Nat. Commun.*, 2013, **4**, 2551.
63 M.-E. Boulon, G. Cucinotta, J. Luzon, C. Degl'Innocenti, M. Perfetti, K. Bernot, G. Calvez, A. Caneschi and R. Sessoli, *Angew. Chem.*, 2013, **125**, 368–372.
64 F. Cimpoesu, N. Dragoe, H. Ramanantoanina, W. Urland and C. Daul, *Phys. Chem. Chem. Phys.*, 2014, DOI: 10.1039/C4CP00953C.
65 V. E. Campbell, H. Bolvin, E. Rivière, R. Guillot, W. Wernsdorfer and T. Mallah, *Inorg. Chem.*, 2014, **53**, 2598–2605.